Probing the Interface in Blends of High and Low Molecular Weight Polystyrene

J. v. Seggern, S. Klotz,* and H.-J. Cantow

Institut für Makromolekulare Chemie, Hermann-Staudinger-Haus, Albert-Ludwigs-Universität Freiburg, D-7800 Freiburg, Federal Republic of Germany.
Received September 14, 1988; Revised Manuscript Received January 9, 1989

ABSTRACT: The interface in a diffusion couple consisting on one side of a blend of high and low molecular weight polystyrene and on the other side of pure high molecular weight polystyrene (N_A and $N_B > N_E$, the entanglement molecular weight) was analyzed. The phase profiles were recorded by scanning infrared microscopy. The initial sharp interface broadened after thermal treatment above the glass transition temperature. Experimental evidence was found that tube renewal influences the mutual diffusion even when both polymers are above the entanglement molecular weight. Assuming a concentration-dependent tracer diffusion coefficient, a semiempirical expression for the mutual diffusion is given. Thus, a qualitative agreement with the prediction of the fast mutual diffusion theory was obtained.

I. Introduction

Diffusion in polymer melts has attracted enormous interest in the past 10 years.[1] Self-diffusion in entangled polymer melts seems to be well understood in terms of reptation theory.[2,3] Despite this, there is still a dispute going on about whether the interdiffusion across the interphase in a diffusion couple of polymer A and polymer B is ruled by the faster or by the slower diffusing species.[4,5] Theoretical inconsistencies seemed to be solved with the elegant experiments of Kramer et al.[6-8] Using forward recoil spectrometry (FRES), they showed that in a diffusion couple of polystyrene and poly(2,6-dimethyl-1,4-phenylene oxide) the interdiffusion was controlled by the faster moving polystyrene. The results could be well fitted with the theoretical approach of Kramer et al.,[5] where a vacancy flux allowed bulk flow to take place. This vacancy flux mechanism was criticized by Brochard and de Gennes,[9] as it would lead to an unacceptable density gradient in the sample. Rather they proposed that up to the reptation time τ_B of the B molecules the shorter chains A swell the longer chains B. This transient swelling is controlled by the diffusion coefficient of the faster A species. The length scale of the swelling regime has usually a magnitude of several micrometers. At times greater than the relaxation time τ_B the interdiffusion should be controlled by the slower B chains. Recently it was shown that the slow theory may merge into the prediction of the fast theory when considering a moving background.[10] Thus, to examine the different theoretical approaches, it is desirable to get experimental data for a length scale of more than a few micrometers.

Very recently Klein et al.[11] presented results, that strongly support that the mutual diffusion or interdiffusion is controlled by the mobility of the faster moving species.[5] They concluded that the appropriate model describing the mutual diffusion in an A/B couple must take into account convective effects, as proposed by Sillescu.[12] The experimental technique used from Klein et al. was infrared microdensitometry (IRM).[13] Nevertheless their experiment has a limited spatial resolution of 60 μm. Thus this technique is limited to polymers with relatively great diffusion coefficients.

In the present study we also used infrared spectroscopy to characterize phase profiles in polymer blends. But with a different sample preparation technique and a measurement procedure the spatial resolution was enhanced up to 10 μm.[14]

The broadening of the interface in a diffusion couple consisting of two identical homopolymers but with very different molecular weights was investigated. For spectroscopic contrast, one of the polymers was deuterated. The schematic representation of our experiment is given in Figure 1. Small cylinders of polymer A and a mixture of polymer A and B were formed by compression molding. A step function was created by pressing both cylinders slightly together. Then the diffusion couple was placed in an exactly fitting container and kept at a particular temperature for different time periods in a vacuum oven. Afterwards a microcut with thickness of 2 μm was taken along the diffusion direction. Then, the microcut was placed under a FT-IR microscope equipped with a computer-controlled movable table. To get the diffusion profile, the microcut was scanned in steps varying between 5 and 15 μm along the diffusion axis with an IR beam size of 10 μm. In this way usually 30–40 complete FT-IR spectra were taken along the interface of the diffusion couple. From the absorbance of the C–D vibration of the different IR spectra and the corresponding x coordinates, the diffusion profiles were directly obtained. In section II the experiments and the investigated materials are described in detail, and in section III results are given and compared with theoretical predictions.

Table I
Molecular Characteristics of Polymers[a]

sample	$10^{-4}M_w$	M_w/M_n	N/N_e
66K	6.6	1.05	4
2000K	1970	1.10	116

[a] The molecular weights were measured by light scattering (M_w) and size exclusion chromatography (M_n). The entanglement length is taken N_e = 17 000.

II. Materials and Methods

The polymers were anionically polymerized polystyrene (PS). The high molecular weight PS-*h*, $M_w = 1.97 \times 10^6$ g/mol, was the hydrogenated polymer and the lower molecular weight PS-*d*, $M_w = 6.6 \times 10^4$ g/mol, was fully deuterated (98%). Samples and characterization are given in Table I.

A mixture of 50 wt % PS-*h* and PS-*d* was made by freeze drying a benzene solution of both components. Afterward the mixture was dried in a vacuum oven for 1 week at 50 °C to remove residual solvent.

A schematic representation of the sample preparation and the measurement procedure is given in Figure 1. Small cylinders (length 3 mm, diameter 2 mm) were formed by slightly pressing the samples for 3 min at 120 °C. The prepared diffusion couple consisted on one side of a 50 wt % mixture of PS-*d* (66K) and PS-*h* (2000K) and on the other side of pure PS-*h* (2000K). The interface was created by pressing the two cylinders together for 5 min at 150 °C. Microcuts were made with an ultramicrotom

0024-9297/89/2222-3328$01.50/0

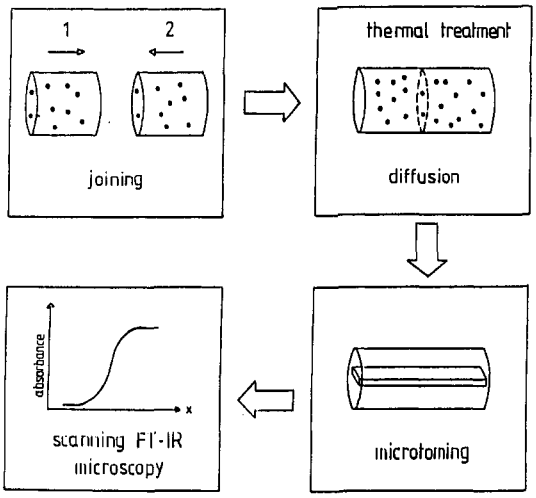

Figure 1. Schematic representation of sample preparation and measurement of the interface profile.

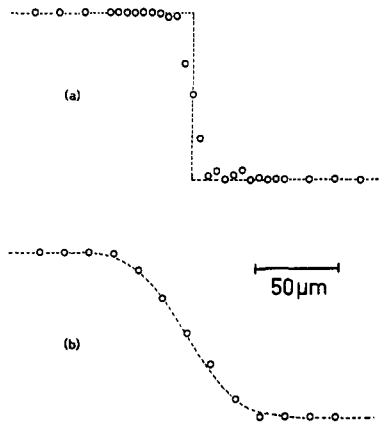

Figure 2. Concentration–distance profile $c(x)$ of a diffusion couple. One side is 50 wt % deuterated-PS ($M_w = 6.6 \times 10^4$)/50 wt % hydrogenated-PS ($M_w = 1970 \times 10^4$) and on the other side, hydrogenated-PS ($M_w = 1970 \times 10^4$): (a) Measured immediately after creation of the step function. The broken line shows the ideal step function. (b) Interface profile after $t = 2.075 \times 10^6$ s at 176 °C. The broken line represents the calculated profile according to eq 1. The interquartile width of the step function (width between $c(x) = c_0/4$ and $3c_0/4$) is ~8 μm, and the width of the broadened profile ~38 μm.

(Reichert-Jung, FRG) and spread on a water surface to prevent themselves from rolling up. The initial broadening was controlled by taking a microcut from the interface and scanning it under the FT-IR microscope along the diffusion direction (scanning infrared microscopy, SIRM). The size of the IR microscope aperture was 10 μm and a step width of 5 and 15 μm was used. Three hundred spectra with a spectral resolution of 8 cm^{-1} were accumulated for each complete IR spectrum to get a sufficient signal-to-noise ratio. Within the range of Beer's law the absorbance is directly proportional to the concentration of the components. In the present case all spectra were in the range of Beer's law, and thus it was concluded that the absorbance of the C–D vibration is directly proportional to the concentration of PS-*d*. The criterion of the specimen regularity and the control of the microcut thickness were performed by the appearance of interference fringes in the IR spectra. The interface profiles were obtained by plotting the normalized absorbance of the C–D vibration versus the coordinates of the corresponding IR spectrum. A typical concentration–distance profile of an initial step function is given in Figure 2a. The broken line indicates the ideal step function. It can be seen from Figure 2a that the initial broadening was about 10 μm. Before each set of diffusion experiments the initial broadening was measured. For the quantitative evaluation of diffusion coefficients the experimental concentration–distance profiles were convoluted with the instrumental resolution function, a Gaussian given by the initial broadening of the interface.

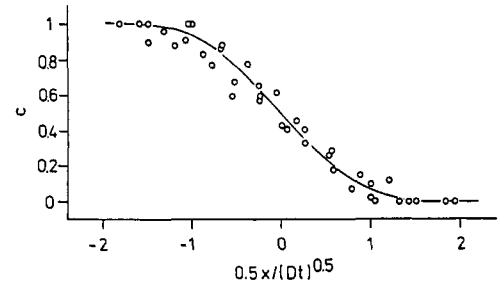

Figure 3. Reduced concentration–distance profile of the diffusion couple 50 wt % PS-*d* (66K) and 50 wt % PS-*h* (2000K)/PS-*h* (2000K) at 150 °C. Data are taken from four independent experiments with varying diffusion times between 0.533×10^6 and 1.760×10^6 s.

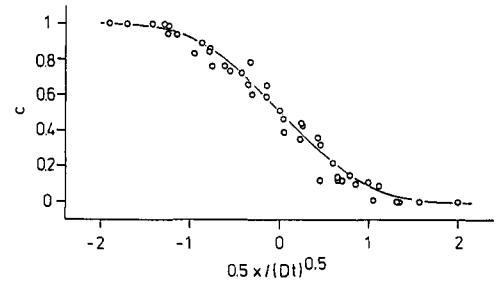

Figure 4. Reduced concentration–distance profile of the diffusion couple 50 wt % PS-*d* (66K) and 50 wt % PS-*h* (2000K)/PS-*h* (2000K) at 176 °C. Data are taken from four independent experiments with varying diffusion times between 0.594×10^6 and 2.075×10^6 s.

Optical examination of the width of the initial interface was performed by filling one side of the diffusion couple with 5 wt % TiO_2. The TiO_2 particles were easy to find in the visible light, and thus a comparison of the position of the experimental interface from IR and from visible inspection could be performed. The midpoint of the interface measured by the SIRM technique was determined from the condition that the diffusion-broadened areas on either side of the midpoint (at $x = 0$) were equal by numerical integration. The position obtained from both techniques agreed within 5 μm.

Figure 2b shows a typical concentration–distance profile after thermal treatment. The interquartile width (the width between $c(x) = c_0/4$ and $3c_0/4$) is about 38 μm compared to 8 μm of the initial interphase. After thermal treatment the samples were quenched below the glass transition temperature ($T_g = 100$ °C). Thus, no artificial broadening occurred during microtoming and scanning the interface.

III. Results and Discussion

Two sets of diffusion experiments were performed. At 150 and 176 °C the interdiffusion of PS-*d* (66K) (blended with 50 wt % PS-*h* (2000K)) into pure PS-*h* (2000K) was measured. For each temperature four experiments with varying periods of diffusion time were carried out. In Figures 3 and 4 all experimental data are shown in reduced concentration–distance graphs.

For an incompressible diffusion couple with a concentration-dependent mutual diffusion coefficient D, the interdiffusion in one dimension is[15]

$$\partial\phi(x,t)/\partial t = \partial/\partial x(D\partial c/\partial x) \quad (1)$$

where ϕ is the volume fraction of one component. The boundary conditions on eq 1 are $\phi = 0$ at $x = -\infty$ and $\phi = 1$ at $x = +\infty$. Theoretical concentration–distance profiles were generated by using a standard iteration procedure[15] with an exponential concentration dependence of D. As the experimental profiles were only slightly concentration dependent, the iteration converged after a few cycles. The

Table II
Tracer Diffusion Coefficients D^* of PS-*d* and PS-*h*[a]

T, °C	$10^{-4}M_w$	D^*, cm²/s
176	6.6	2.0×10^{-12}
176	2000	1.9×10^{-15}

[a] Data were taken from ref 16 and 17.

solid lines in Figures 3 and 4 depict the fitted interface profiles, calculated by eq 1.

First, it is surprising that the profiles are only slightly concentration dependent. For a highly asymmetric diffusion couple such as in the present case, one would expect a highly asymmetric interface profile as well. This apparent inconsistency will be discussed in detail in the next section.

Theory predicts[4,5] that for a diffusion couple of low and high molecular weight polymers, A and B, which are both well above the entanglement molecular weight (polymerization indices N_A, $N_B > N_E$ where N_E is the number of monomers/entanglement, assumed to be the same for A and B) the chains move by reptation. Introducing a vacancy flux the interdiffusion of A and B across the interface is given by[5]

$$D_1 = [D_A^* N_A \phi_B + D_B^* N_B \phi_A][\phi_B/N_A + \phi_A/N_B - 2\phi_A\phi_B\chi] \quad (2)$$

where diffusion is controlled by the faster moving shorter chains. Another approach retains the incompressibility condition and results in the expression[4]

$$D_2 = [\phi_B/(D_A^* N_A) + \phi_A/(D_B^* N_B)]^{-1}[\phi_B/N_A + \phi_A/N_B - 2\phi_A\phi_B\chi] \quad (3)$$

where the mutual diffusion of both chains is coupled and essentially controlled by the slower species. A recent generalization of the latter theory that considers the moving background with a distinct velocity finally leads to the result of the fast theory.[10] It is evident from eq 2 and 3 that the interdiffusion should be highly concentration dependent when $N_A \ll N_B$. In Figure 5 a representative experimental profile and the calculated profiles from eq 2 and 3 are given. The tracer diffusion coefficients D_A^* and D_B^* were taken from the literature[16,17] and are listed in Table II. In Figure 5a, the slow theory completely fails in describing the broadened interface, whereas the fast theory (Figure 5b) predicts the broadening at the high molecular weight side of the diffusion couple quite well (right-hand side in Figure 5b). Nevertheless, one finds a marked discrepancy at the left-hand side, where the long chains diffused into the blend of the short and the long PS chains. Despite both chains being above the entanglement molecular weight, the long chains move into a matrix where tube renewal may influence the mutual diffusion and thus the broadening of the interface. Tracer diffusion experiments of Green et al.[18] showed that tube renewal may be important in the present case. Thus, to get a more quantitative description of the present experiments, eq 2 and 3 have to be modified to allow for tube renewal.

Recent experiments of Kramer et al.[19] and Smith et al.[20] investigated the diffusion in blends, where one component was too short to make entanglements. The experimental diffusion coefficients strongly depended on the matrix molecular weight (or on the concentration of the short chains) when the jump time for a primitive path step approached the relaxation time of the constrainst built up by the surrounding matrix. Kramer et al.[19] developed a

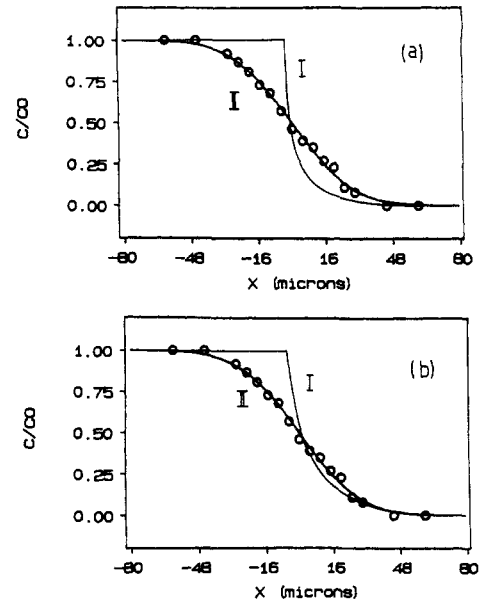

Figure 5. (a) Open circles show the experimental concentration–distance profile of a 50 wt % PS-*d* (66K) and 50 wt % PS-*h* (2000K)/PS-*h* (2000K) diffusion couple at 176 °C and 1.210×10^6 s. Curve II was fitted with eq 1; curve I was calculated from eq 2 where the slow species controls the mutual diffusion. (b) Open circles and curve II have the same meaning as in Figure 5a. Curve I was calculated from eq 3 where the fast species controls the mutual diffusion.

semiempirical concentration dependence for the tracer diffusion coefficient:

$$D^*(\phi) = D_R/a_c(\phi)(1/\phi + \alpha_{CR} M M_E^2/P^3\phi^3) \quad (4)$$

where

$$\alpha_{CR} = (48/25)z(12/\pi^2)^{z-1}$$

D_R denotes the reptation diffusion coefficient for a tracer chain M, P is the molecular weight of P chains in the matrix, and $a_c(\phi)$ considers the change of the glass transition when longer chains are diluted with shorter chains. $a_c(\phi)$ may be expressed in terms of the WLF shift factor a_T,[19,21] and z is the number of constraints defining the tube at any cross section.[24] The main assumptions of eq 4 are that only the long chains can form constraints and that $M_E(\phi)$ is inversely proportional to ϕ. The latter assumption was reasoned by the experimentally observed concentration dependence of the viscoelastic response functions.[22] However, Smith et al.[20] found $D \sim c^{-2.2}$ in highly concentrated solutions of poly(propylene oxide) in oligomeric propylene oxide. In a recent theoretical treatment Rubinstein et al.[23] argued that the plateau modulus $G_N^0 \sim \phi^\alpha$ with $\alpha = 3$. This implies a stronger concentration dependence of the entanglement density and thus of the diffusion coefficient. Due to this inconsistency we refrain from the assumption that $M_E(\phi) \sim c^{-1}$ in eq 4 and write $M_E(\phi) \sim c^{-\beta}$, where β is now a fitting parameter. As the short chains in the present case also contribute to the constraints, we write for the matrix molecular weight P in eq 4

$$P = w_A M_A + w_B M_B \quad (5)$$

where w_A and w_B are the weight fractions of polymer A and B, respectively. Thus, eq 4 can be modified, and one obtains

$$D^*(\phi) = D_R/a_c(\phi)(1/\phi^\beta + M M_E^2/P^3\phi^{3\beta}) \quad (6)$$

From eq 6 the concentration dependence of the tracer

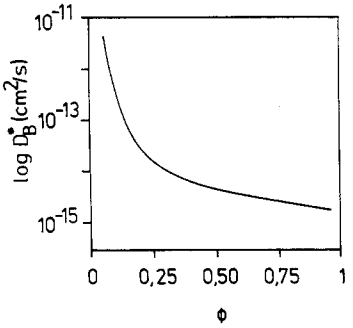

Figure 6. Tracer diffusion coefficient D_B^* of the high molecular weight polymer B versus the volume fraction of B in the matrix, M_A = 66 000 and M_B = 2 000 000. The line was calculated from eq 6.

diffusion coefficient $D_B^*(d)$ of the long chains in a matrix of varying concentration of A (66K) and B (2000K) molecules can be calculated (Figure 6). The constraint release parameter was z = 3 (ref 24) and the exponent b = 1.5. The tracer diffusion coefficient of B is given in Table II, and the entanglement molecular weight of the undiluted matrix M_E = 18000. It can be seen from Figure 6 that the tracer diffusion coefficient of the long chains B is enhanced with increasing concentration of the shorter chains A.

Equations 2 and 3 can now be modified by inserting eq 6 for D_B^*, where tube renewal is supposed to influence the mutual diffusion, leading to

$$D_1 = [D_A^* N_A \phi_B + D_B^*(\phi) N_B \phi_A][\phi_B/N_A + \phi_A/N_B - 2\phi_A\phi_B\chi] \quad (7)$$

and for the slow theory

$$D_2 = [\phi_B/(D_A^* N_A) + \phi_A/(D_B^*(\phi) N_B)]^{-1}[\phi_B/N_A + \phi_A/N_B - 2\phi_A\phi_B\chi] \quad (8)$$

In the present case D_A^* was assumed to be constant, as it is unlikely that tube renewal influences the diffusion of the faster chains A.[17]

In Figure 7 the mutual diffusion was calculated from eq 7 and 8. Again, the experimental data and the best fit from eq 1 are shown. The broadening at the high molecular weight side of the interface did not change significantly, whereas the left side is now broadened by tube renewal. Comparison with Figure 5 reveals the importance of tube renewal when a long chain moves into a matrix with lower molecular weight. The fast theory fits the experimental data qualitatively well, whereas the slow theory fails. With the semiempirical relation of the concentration dependence of D_B^*, one should not expect quantitative agreement with the experiments. But, in a first approximation one finds a satisfying qualitative agreement.

The present experiments reveal that tube renewal may be an important factor when a long polymer chain is diffusing into a matrix of significantly lower molecular weight, despite both polymers being above the entanglement molecular weight. Even in diffusion couples where both polymers have more than 21 times the entanglement molecular weight, one can find some experimental evidence for tube renewal (see in Figures 3 and 4 of ref 11 at the lower molecular weight side of the diffusion couples).

This is not surprising as recent analysis of the relaxation behavior of highly entangled polymer mixtures via viscoelastic response functions focused attention to tube renewal effects. Graessley et al.[25] measured the stress relaxation in entangled low and high molecular weight mixtures of polybutadiene over the complete concentration range. The frequency and the shape of the modulus peaks

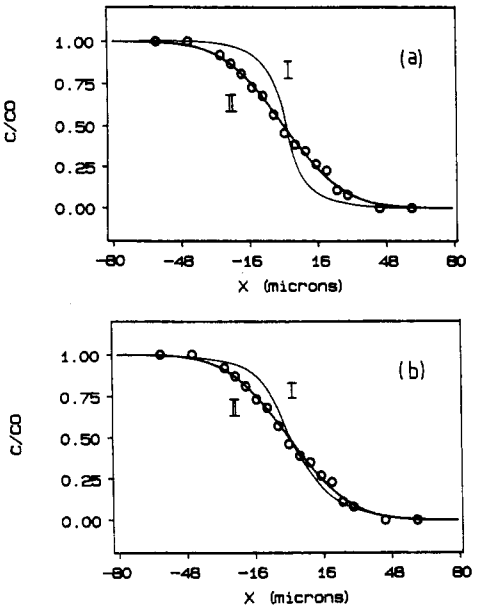

Figure 7. (a) Open circles and curve II have the same meaning as in Figure 5a. Curve I was calculated from the modified slow theory eq 8 considering reptation and tube renewal. (b) Open circles and curve II have the same meaning as in Figure 5a. Curve I was calculated from the modified fast theory eq 7 considering reptation and tube renewal.

changed significantly with the mixture composition. In a later theoretical treatment of their data, Graessley[26] showed that this behavior may be explained only by considering tube renewal in the relaxation process. In a detailed theoretical analysis Rubinstein et al.[23] showed that Graessley's data may be well fitted by using the Marrucci–Viovy theory.[27,28] They pointed out that tube renewal and tube length fluctuations must be taken into account even in mixtures where $M_w/M_E > 21$ for the lower molecular weight polymer. A striking example where tube renewal competes with reptation even in ultrahigh molecular weight homopolymer melts was given by Graessley et al.[29] It was shown that the theoretical zero-shear viscosity fits the experimental data only when tube renewal was considered.

From these arguments it seems evident that tube renewal is important in the understanding of the present diffusion experiments. With a concentration-dependent tracer diffusion coefficient a semiempirical approach for the mutual diffusion was given. The shape of the interface profiles of the present experiments was qualitatively described by the modified fast theory. The slow theory failed in describing the profiles even when tube renewal was taken into account.

Acknowledgment. J.v.S. thanks the Graduiertenkolleg Polymerwissenschaften at the University of Freiburg. S.K. thanks R. Stadler for helpful comments and suggestions. The financial support of the Bundesministerium für Forschung und Technologie (BMFT) is gratefully acknowledged.

Registry No. PS, 9003-53-6.

References and Notes

(1) Klein, J. In *Encyclopedia of Polymer Science and Engineering*, 2nd ed.; Wiley: New York, 1987; Vol. 9, Macromolecular Dynamics.
(2) de Gennes, P.-G. *Scaling Concepts in Polymer Physics*; Cornell University Press: Ithaca, NY, 1979.
(3) Doi, M.; Edwards, S. F. *The Theory of Polymer Dynamics*; Oxford University Press: Oxford, 1986.
(4) Brochard, F.; Jouffroy, J.; Levinson, P. *Phys. Lett.* **1983**, *44*, L-455.

(5) Kramer, E. F.; Green, P. F.; Palmstrom, C. F. *Polymer* **1984**, *25*, 473.
(6) Composto, R. J.; Mayer, J. W.; Kramer, E. J.; White, D. *Phys. Rev. Lett.* **1986**, *57*, 1312.
(7) Composto, R. J.; Kramer, E. J.; White, D. M. *Macromolecules* **1988**, *21*, 2580.
(8) Composto, R. J.; Kramer, E. J.; White, D. *Nature* **1987**, *328*, 1980.
(9) Brochard, F.; de Gennes, P.-G. *Europhys. Lett.* **1986**, *1*, 221.
(10) Brochard-Wyart, F. *C. R. Acad. Sci. Ser. 2* **1987**, *305*, 657.
(11) Jordan, E. A.; Ball, R. C.; Donald, A. M.; Fetters, L. F.; Jones, R. A. L.; Klein, J. *Macromolecules* **1988**, *21*, 235.
(12) Sillescu, J. *Makromol. Chem. Rapid Commun.* **1984**, *5*, 519.
(13) Klein, J.; Briscoe, B. J. *Proc. R. Soc. London* **1979**, *365*, 53.
(14) Klotz, S.; DeAraujo, M. A.; Cantow, H.-J. *Proc. ACS Div. Polym. Mater.: Sci. & Eng.* **1988**, *58*, 827.
(15) Crank, J. *The Mathematics of Diffusion*; Clarendon Press: Oxford, 1975.
(16) Composto, R. J. Ph.D. Thesis, Cornell University, 1987.
(17) Green, P. F.; Kramer, E. F. *Macromolecules* **1986**, *19*, 1108.
(18) Green, P. F.; Mills, P. J.; Palmstrom, C. J.; Mayer, J. W.; Kramer, E. J. *Phys. Rev. Lett.* **1984**, *53*, 2145.
(19) Tead, S. F.; Kramer, E. J. *Macromolecules* **1988**, *21*, 1513.
(20) Smith, B. A.; Mumby, S. J.; Samulski, E. T.; Yu, L. P. *Macromolecules* **1986**, *19*, 470.
(21) von Meerwall, E.; Amis, E. J.; Ferry, J. D. *Macromolecules* **1985**, *18*, 260.
(22) Graessley, W. W. *Polymer* **1980**, *21*, 258.
(23) Rubinstein, M.; Helfand, E.; Pearson, D. S. *Macromolecules* **1987**, *20*, 822.
(24) Graessley, W. W. *Adv. Polym. Sci.* **1982**, *47*, 67.
(25) Struglinski, M. J.; Graessley, W. W. *Macromolecules* **1985**, *18*, 2630.
(26) Graessley, W. W.; Struglinski, M. J. *Macromolecules* **1986**, *19*, 1754.
(27) Marrucci, M. J. *J. Poly. Sci., Polym. Phys. Ed.* **1985**, *23*, 159.
(28) Viovy, J. L. *J. Phys. (Les Ulis, Fr.)* **1985**, *46*, 847.
(29) Colby, R. H.; Fetters, L. J.; Graessley, W. W. *Macromolecules* **1987**, *20*, 2226.

Scattering Behavior of Wormlike Star Macromolecules

Klaus Huber and Walther Burchard*

Institute of Macromolecular Chemistry, University of Freiburg, 7800 Freiburg i.B., West Germany. *Received November 23, 1988*

ABSTRACT: Calculations by Mansfield and Stockmayer on the radius of gyration of wormlike star molecules have been extended to the angular dependence of the corresponding scattering functions $P(q)$. Analytical expressions could be derived on the basis of the Koyama theory for wormlike chains if the arms are freely hinged at the star center ("combinatorial star" approximation). The results are compared with Monte Carlo calculations and small-angle neutron-scattering measurements from 12-arm polystyrene stars in a Θ solvent.

Introduction

Star-branched macromolecules continue to be of great interest to polymer scientists. This architecture occurs in every type of network as an elementary substructure, and understanding the conformational behavior may help to improve present knowledge about the conformation of networks. Up to now Gaussian chain statistics have been assumed.[1,2] However, even under idealized thermodynamic conditions, i.e. at vanishing second-virial coefficient, $A_2 = 0$, the chains exhibit no ideal flexibility. Chain stiffness of the arms and a defined angle between the initial tangents of the arms at the star center exert influence on the global and internal structure of these star molecules.

Particle scattering functions of realistic models with fixed angles at the star center are difficult to treat analytically. Therefore, Monte Carlo simulations applying different concepts were recently carried out.[3,4] These simulations allowed the numerical calculation of the static and dynamic scattering behavior. Such simulations are time-consuming and cannot be easily extended to more complex architectures, e.g. multiply branched clusters. Analytical equations will facilitate the derivation of scattering curves and the interpretation of experimental data from these more complex structures.

A few years ago Mansfield and Stockmayer[5] derived a general relationship for the mean-square radius of gyration of wormlike star molecules. They assumed wormlike arms with and without a certain angle correlation among the arms at the center. Two cases were treated explicitly. In the one case the angles were fixed at the star center, and in the other the arms were freely jointed. In the following we call the second case the "broken wormlike star", and we show that the particle scattering factor of this structure can be calculated analytically on the basis of the Koyama approximation[6] for linear chains.

Three chain models for the arms of the stars are applied, i.e. the Gaussian model, the rodlike model, and the wormlike model. A combinatorial concept consisting of *two* different approaches is used to derive analytical expressions for the particle scattering factor of these star models. To check the validity of the wormlike chain model, the analytical expressions are compared with two different types of data: (i) Monte Carlo results on polymethylene 12-arm stars, based on Flory's model of rotational isomeric states[7] (RIS); (ii) small-angle neutron-scattering (SANS) data on 12-arm polystyrene stars in dilute solution of cyclohexane-*d*.

Samples and Methods

The Monte Carlo procedure on polymethylene was previously described in detail.[8] For both combinatorial approaches of Monte Carlo stars, we could use stored histograms of the intraparticular distance distribution for linear chains. In the combinatorial approach, where two arms are connected to a continuous linear chain, the same data as in ref 4 were used.

Experimental data are those of neutron-scattering experiments from two 12-arm polystyrene star samples in the Θ-solvent cyclohexane-*d*, which were already presented in ref 4.

Particle-scattering functions of wormlike stars based on the approximation of Koyama[6] were calculated with the aid of the integration subroutine DCADRE of the IMSL Library.

Combinatorial Stars

The idea of combinatorial stars consists in the use of the particle-scattering factors of *linear* chains, $P_N(q)$ for one arm and $P_{2N}(q)$ for two connected arms, and these particle-scattering factors are weighed then according to their

0024-9297/89/2222-3332$01.50/0